

## HIGH-FREQUENCY CHANGES IN THE ORIENTATION OF NEMATIC LIQUID CRYSTALS IN RADIO FREQUENCY CROSSED ELECTRIC FIELDS

V. M. Klement'ev, S. I. Trashkeev,  
P. A. Statsenko, and T. D. Valinurov

UDC 532.783

*The orientational dynamics of the director of a nematic liquid crystal located in radio frequency crossed electric fields were studied by numerical calculations and experimentally. This system is shown to be a physical object of nonlinear dynamics. Depending on the parameters of the problem, the following types of states of the director were observed: stationary (an analog of the nonthreshold Freedericksz transition), periodic, quasiperiodic (multimode), and stochastic of the strange attractor type. In the calculations, all states were obtained by solving a deterministic system of two time-dependent nonlinear differential equations of the first order with no electrohydrodynamic terms. All types of solutions obtained, including stochastic ones, were observed experimentally.*

**Key words:** liquid crystals, attractor, stochastics, Freedericksz effect.

**Introduction.** The electrooptic properties of liquid crystals (LCs) have been adequately studied and described in numerous papers [1–4]. Liquid-crystal media have found wide application in the area of data display [2]. Such applications are based on the reorientation effect of the LC director (the direction of the long axes of LC molecules averaged over thermal fluctuations) and the crystal optic axis under the action of low-voltage electric fields — the Freedericksz effect [1]. The time characteristics of Freedericksz reorientation, as a rule, are high and are approximately 10–100 msec for nematic LCs (NLCs). The low response accompanying electrooptic variation in NLCs is due to the high rotational viscosity (0.01–0.1 Pa · sec) [3], which is characteristic of almost all liquid crystals. Therefore, it is assumed that the director reorientation is determined by the viscosity and the effective value of the alternating electric field irrespective of its frequency. In view of this, it is concluded that high-frequency orientation processes are impossible in LCs [5].

The objective of the present work was to study the orientational behavior of the NLC director in electric fields consisting of several components with different directions and frequencies. It is shown that the dynamics of the involved processes is much more difficult than “simple” Freedericksz reorientation [1]. The motion of the director begins to depend on the amplitudes, frequencies, and phases of the applied voltage and can be undamped multifrequency (quasiperiodic) oscillating or rotational changes of the orientation up to stochastic regimes of the strange attractor type. The dynamics of the involved processes is not a consequence of electrohydrodynamic (EHD) instability [4] although in some cases the observed phenomena are accompanied by macroscopic liquid flows. The theoretical conclusions have been supported by data of preliminary experiments.

The possibility of stochastization of the NLC orientation in the absence of EHD effects was first indicated in a paper [6], in which the interaction of a NLC with an oblique light wave of the ordinary type was studied experimentally. Later, the possibility of occurrence of quasiperiodic and multimode regimes in models describing experiments [6] was detected in a study [7] of deterministic equations using numerical calculations. This phenomenon was also studied in [8].

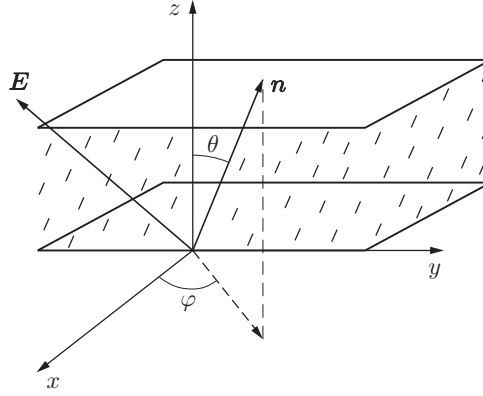


Fig. 1. Geometry of interaction of the NLC director with an arbitrarily directed electric field.

Although the model used in the present work is more adequate to the case of interaction of a NLC with radio frequency alternating electric fields, it can also be treated as a certain approximation for describing harmonic generation in light coherent fields. More precisely, this model is a first iteration that ignores the self-effect of transmitted waves and is realizable for  $|\Delta\mathbf{k}| \ll 1/d$ , where  $|\Delta\mathbf{k}|$  is the maximum spread of wave vectors in the medium and  $d$  is the characteristic dimension of the orientation change.

**Equations of Motion.** To derive dynamic equations, we choose the interaction geometry (Fig. 1) in Cartesian coordinates  $\mathbf{r} = (x, y, z)$ . The following notation is used:  $\mathbf{E} = \mathbf{E}(t, \mathbf{r})$  is the real vector of the electric field in the crystal;  $\mathbf{n} = \mathbf{n}(t, \mathbf{r})$  is the unit vector (director);  $\theta$  and  $\varphi$  are the polar and azimuthal angles, which are linked to  $\mathbf{n}$  by the relation

$$\mathbf{n} = (n_x, n_y, n_z) = (\sin \theta \cos \varphi, \sin \theta \sin \varphi, \cos \theta).$$

For the further consideration, it is convenient to introduce auxiliary unit vectors orthogonal to  $\mathbf{n}$ :

$$\mathbf{m} = (m_x, m_y, m_z) = \frac{\partial \mathbf{n}}{\partial \theta} = (\cos \theta \cos \varphi, \cos \theta \sin \varphi, -\sin \theta),$$

$$\mathbf{p} = (p_x, p_y, p_z) = \frac{1}{\sin \theta} \frac{\partial \mathbf{n}}{\partial \varphi} = (-\sin \varphi, \cos \varphi, 0),$$

$$(\mathbf{n}\mathbf{m}) = 0, \quad (\mathbf{n}\mathbf{p}) = 0, \quad (\mathbf{m}\mathbf{p}) = 0.$$

For NLCs, the free-energy density  $F$  is written as [1]

$$F = \frac{1}{2} \left[ K_1 (\operatorname{div} \mathbf{n})^2 + K_2 (\mathbf{n} \operatorname{rot} \mathbf{n})^2 + K_3 (\mathbf{n} \times \operatorname{rot} \mathbf{n})^2 \right] - \frac{\varepsilon_a}{8\pi} (\mathbf{n}\mathbf{E})^2. \quad (1)$$

In the functional (1),  $K_1, K_2$ , and  $K_3$  are the Frank elastic constants and  $\varepsilon_a = \varepsilon_{||} - \varepsilon_{\perp}$ , where  $\varepsilon_{||}$  and  $\varepsilon_{\perp}$  are the parameters of the permittivity matrix, which is expressed in terms of the Cartesian components of the director  $n_i$  by

$$\varepsilon_{ij} = \varepsilon_{\perp} \delta_{ij} + \varepsilon_a n_i n_j, \quad i, j = x, y, z \quad (2)$$

( $\delta_{ij}$  is the Kronecker delta).

For simplification, we assume that in the examined range of the electric-field frequency  $\mathbf{E}$ , the values of the material parameters  $K_i$ ,  $\varepsilon_{||}$ , and  $\varepsilon_{\perp}$  are constant.

In the one-dimensional case where all sought quantities depend only on the  $z$  coordinate and time  $t$ , expression (1) is written as

$$F = \frac{1}{2} \left[ f \left( \frac{\partial \theta}{\partial z} \right)^2 + g \left( \frac{\partial \varphi}{\partial z} \right)^2 - \frac{\varepsilon_a}{4\pi} (\mathbf{n}\mathbf{E})^2 \right], \quad (3)$$

$$f = f(\theta) = K_1 \sin^2 \theta + K_3 \cos^2 \theta, \quad g = g(\theta) = \sin^2 \theta (K_2 \sin^2 \theta + K_3 \cos^2 \theta).$$

Variation of the functional (3) taking into account the relaxation terms yields a system of two nonlinear equations for  $\theta$  and  $\varphi$ :

$$\begin{aligned}\gamma \frac{\partial \theta}{\partial t} &= f \frac{\partial^2 \theta}{\partial z^2} + \frac{1}{2} \left[ f_\theta \left( \frac{\partial \theta}{\partial z} \right)^2 + g_\theta \left( \frac{\partial \varphi}{\partial z} \right)^2 \right] + \frac{\varepsilon_a}{4\pi} (\mathbf{nE})(\mathbf{mE}), \\ \gamma \sin^2 \theta \frac{\partial \varphi}{\partial t} &= \frac{\partial}{\partial z} \left( g \frac{\partial \varphi}{\partial z} \right) + \frac{\varepsilon_a}{4\pi} \sin \theta (\mathbf{nE})(\mathbf{pE}),\end{aligned}\tag{4}$$

where  $f_\theta = \partial f / \partial \theta$ ,  $g_\theta = \partial g / \partial \theta$ , and  $\gamma$  is the viscous parameter of the NLC. In the derivation of (4), the flexoelectric components and the possibility of hydrodynamic flows were ignored.

The constitutive equations (4) need to be supplemented by boundary conditions at the points  $z = 0, L$  ( $L$  is the crystal thickness). Following [4], these conditions were chosen in the form

$$\left[ K \frac{\partial \theta}{\partial z} \pm a_\theta \theta \right]_{z=0,L} = b_\theta, \quad \left[ K \frac{\partial \theta}{\partial z} \pm a_\varphi \varphi \right]_{z=0,L} = b_\varphi,\tag{5}$$

where the plus and minus refer to  $z = 0$  and  $z = L$ , respectively,  $K$  is the averaged Frank constant, and the parameters  $a_\theta$ ,  $a_\varphi$ ,  $b_\theta$ , and  $b_\varphi$  generally depend on the surface energy density of the bonding of the director to the bounding planes, flexoelectric coefficients, and electric fields.

To close the system, Eqs. (4) should be supplemented by the Maxwell equations relating the electric fields to the orientation  $\mathbf{n}$ . Ignoring the conductivity of the medium, for the radio frequency range inside the sample, we write

$$\operatorname{div}(\hat{\varepsilon}\mathbf{E}) = 0, \quad \operatorname{rot} \mathbf{E} = 0.\tag{6}$$

Here  $\hat{\varepsilon}$  is the permittivity matrix (2). In the one-dimensional case, Eqs. (6) subject to (2) become

$$\frac{\partial}{\partial z} \left[ \varepsilon_\perp E_z + \varepsilon_a n_z (\mathbf{nE}) \right] = 0, \quad \frac{\partial E_x}{\partial z} = \frac{\partial E_y}{\partial z} = 0.\tag{7}$$

Equations (7) are trivially integrated, and the electric fields inside the crystal are determined uniquely from specified field magnitudes. With addition of the corresponding initial conditions on the orientation angles

$$\theta(0, z) = \theta_0(z), \quad \varphi(0, z) = \varphi_0(z)$$

system (4) with boundary conditions (5) and the solution following from (7) becomes a closed system that describes the interaction of NLCs with arbitrarily directed alternating electric fields in the one-dimensional case.

For fairly strong electric fields far exceeding the threshold magnitudes for Fredericksz reorientation [1],

$$|\mathbf{E}|^2 \gg E_{\text{th}}^2 = 4\pi^3 K / (L^2 \varepsilon_a)$$

( $K$  is the averaged Frank elastic constant), the boundary conditions and spatial relations can be ignored in some cases. Conditions that allow one to ignore coordinate dependences will be discussed below. After appropriate simplifications, Eqs. (4) and (7) become a system of ordinary differential equations which depend only on time:

$$\begin{aligned}\gamma \frac{d\theta}{dt} &= \frac{\varepsilon_a}{4\pi} (\mathbf{nE})(\mathbf{mE}), \quad \gamma \sin \theta \frac{d\varphi}{dt} = \frac{\varepsilon_a}{4\pi} (\mathbf{nE})(\mathbf{pE}), \\ E_z &= \frac{\varepsilon_{||} E_z^{\text{ex}} - \varepsilon_a \cos \theta \sin \theta (E_x \cos \varphi + E_y \sin \varphi)}{\varepsilon_\perp + \varepsilon_a \cos^2 \theta}, \quad E_x = E_x^{\text{ex}}, \quad E_y = E_y^{\text{ex}}\end{aligned}\tag{8}$$

$[\theta = \theta(t)$  and  $\varphi = \varphi(t)$  are angle functions at the center of the sample ( $z = L/2$ )]. Here we assume the initial homeotropic orientation  $\theta(0) = 0$  and spatial homogeneity of the electric field  $\mathbf{E} = \mathbf{E}(t)$ ;  $\mathbf{E}^{\text{ex}}(t)$  is the specified magnitude of the electric field in vacuum.

**Electric Field Lying in One Plane. Analytical Solution.** It seems impossible to solve systems (8) and (4) analytically, and, hence, this will be done numerically. We first consider some particular cases that allow for analytical solutions.

If the electric field vector  $\mathbf{E} = \mathbf{E}(t)$  lies in one plane, for example,  $(x, y)$ , then, for  $\theta \equiv \pi/2$ ,  $\varphi = \varphi(t)$ , and  $\mathbf{E} = \{E_x(t), E_y(t), 0\}$  instead of system (8), we obtain one equation for the azimuthal angle  $\varphi$  ( $E_z \equiv 0$ ):

$$\gamma \frac{d\varphi}{dt} = \frac{\varepsilon_a}{4\pi} (E_x \cos \varphi + E_y \sin \varphi)(-E_x \sin \varphi + E_y \cos \varphi).\tag{9}$$

In the case of a harmonic dependence  $\mathbf{E}(t) = A\{\sin(\omega t + \psi_x), \sin(\omega t + \psi_y), 0\}$ , namely a rotating (circular) field  $E_x = A \cos \omega t$ ,  $E_y = \sin \omega t$  ( $\psi_x = \pi/2$ ,  $\psi_y = 0$ ), we obtain

$$\frac{d\varphi}{dt} = -\frac{\varepsilon_a A^2}{8\pi\gamma} \sin[2(\varphi - \omega t)]. \quad (10)$$

An identical equation can be written for the polar angle  $\theta$  when considering the case of an alternating electric field lying, for example, in the plane  $(x, z)$ . For this, it is necessary to set  $\theta = \theta(t)$ ,  $\varphi \equiv 0$ , and  $\mathbf{E} = \{E_x(t), 0, E_z(t)\}$  and to ignore the additive to the  $z$  component of the field that is proportional to  $\varepsilon_a$  and follows from condition (7).

Equation (10) is integrated analytically. We first make the replacement  $\alpha = 2(\varphi - \omega t)$  and write (10) as

$$\frac{d\alpha}{d\tau} = -2(1 + \delta \sin \alpha).$$

As a result, we obtain the solution

$$\varphi(\tau) = \begin{cases} \tau - \arctan[\delta + \Omega \tan \Omega(\tau - C)], & \delta^2 < 1, \quad \Omega^2 = 1 - \delta^2, \\ \tau - \arctan[(\tau - 1 - C)/(\tau - C)], & \delta^2 = 1, \quad \Omega^2 = 0, \\ \tau - \arctan[\delta - \Omega \tanh \Omega(\tau - C)], & \delta^2 > 1, \quad \Omega^2 = \delta^2 - 1, \end{cases} \quad (11)$$

where  $\tau = \omega t$  is dimensionless time and  $\delta = \varepsilon_a A^2 / (8\pi\gamma\omega)$ . It should be noted that relation (11) contains a term linear in time that leads to continuous (on the average) rotation of the director.

For comparison, we give the solution of Eq. (9) for a field  $\mathbf{E}$  with a constant direction in space:  $E_x = A \sin \omega t$ ,  $E_y = A \cos \omega t$  ( $\psi_x = \psi_y = 0$ ). Equation (9) implies

$$\frac{d\varphi}{dt} = \frac{\varepsilon_a A^2}{4\pi\gamma} \sin^2 \omega t \cos 2\varphi. \quad (12)$$

Equation (12) is also easy to integrate, and its solution is written as

$$\varphi = -(\pi/4) \pm \arctan\{C \exp[\delta(2\tau - \sin 2\tau)]\}, \quad (13)$$

where  $C$  is the integration constant; the dimensionless time  $\tau$  and the parameter  $\delta$  are determined as in the previous case. Relation (13) describes the nonthreshold Fredericksz reorientation in an alternating electric field.

Let us consider the deviations of the director from the mean stationary state  $\Delta\varphi = \varphi(t) - \varphi_{st}$  for both versions of field configuration in the steady-state regime ( $\tau \rightarrow \infty$ ) and under the condition  $\delta^2 \ll 1$  or  $\omega \gg \varepsilon_a A^2 / (8\pi\gamma)$ . For a rotating field, from (11) we obtain the relation

$$\Delta\varphi \approx \frac{\varepsilon_a A^2}{8\pi\gamma\omega} \sin 2\omega t + \frac{1}{\omega} \left( \frac{\varepsilon_a A^2}{8\pi\gamma} \right)^2 t, \quad (14)$$

which contains oscillating terms and terms increasing linearly in time. For the second case, from (13) we have

$$\Delta\varphi \approx \frac{\varepsilon_a A^2}{4\pi\gamma\omega} \exp\left(-\frac{\varepsilon_a A^2}{4\pi\gamma} t\right) \sin^2 \omega t. \quad (15)$$

From the asymptotic relation (14) and (15), it is obvious that the oscillation amplitude of the director is finite in time in the case of a circular field and tends exponential to zero as  $t \rightarrow \infty$  in a field with a constant direction. The undamped oscillating behavior of the orientation, as well as the continuous rotation of the director with a frequency proportional to the supplied voltage to the fourth power is a qualitative feature that distinguishes the case (14) from the Fredericksz transition (15).

The possibility of continuous rotation of the director was found and studied in [9] for the interaction of a homeotropically aligned NLC with a circularly polarized light wave. Taking into account the approximations stipulated in the introduction, solution (14) considered in the present paper is largely equivalent to the results given in [9].

Figure 2 shows curves of  $\varphi(\tau)$  for both field configurations and different values of  $\delta$ . Curve 1 is the reorientation in a field with a constant direction, and curve 4 is obtained by solving the partial differential equations (4) for the center of the sample  $\varphi(\tau) \equiv \varphi(\tau, L/2)$ . The spatial dependence implied by the finiteness of the elastic forces

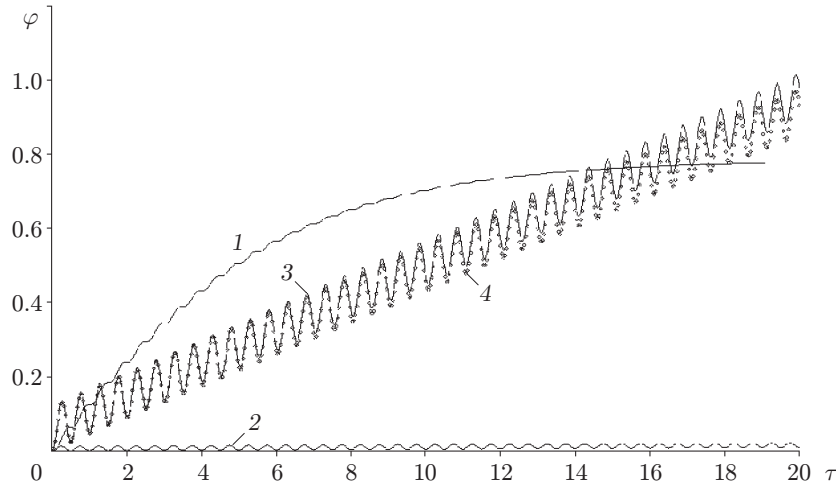


Fig. 2. Azimuthal orientation angle of the 5SV NLC director versus the dimensionless time  $\tau$  for the case of an electric field lying in the plane  $(x, y)$ : 1)  $\psi_x - \psi_y = 0$  and  $\delta = 0.5$ ; 2)  $\psi_x - \psi_y = \pi/2$  and  $\delta = 0.3$ ; 3)  $\psi_x - \psi_y = \pi/2$  and  $\delta = 3$ ; 4)  $\psi_x - \psi_y = \pi/2$  and  $\delta = 3$  (solution taking into account the elasticity of the medium).

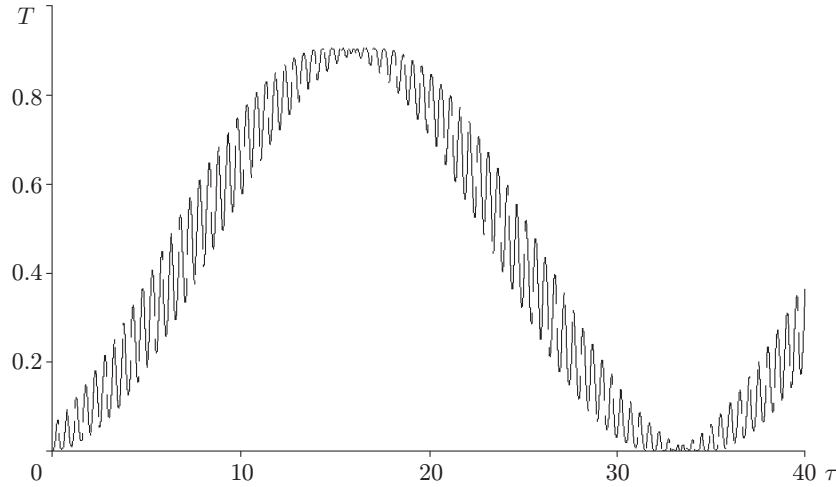


Fig. 3. Transmission function versus dimensionless time for a rotating field with  $\psi_x - \psi_z = \pi/2$  and  $\delta = 3$ .

acting in the NLC is thus taken into account. Boundary conditions (5) were chosen for the homeotropic orientation and had the form

$$\theta|_{0,L} = 0, \quad \frac{\partial \varphi}{\partial z}|_{0,L} = 0.$$

The field amplitude was twice the threshold value ( $|\mathbf{E}| = 2E_{\text{th}}$ ). As can be seen from comparison of curves 3 and 4, the difference lies only in a small change in the slope of the average values of  $\varphi$  to the  $\tau$  axis. Figure 3 shows the calculated transmission function  $T(\tau)$  in the crossed polarizers of a NLC (for a 5SV sample of thickness  $L = 150 \mu\text{m}$  ignoring elasticity) in a rotating field with  $\delta = 3$ . The smooth envelope  $T(\tau)$  following from (11) is caused by the director rotation. The high-frequency component which also follows from (11) is defined by the oscillating term.

In the case of a circular field in the plane  $(x, z)$ , the solutions taking into account and ignoring the elasticity of the NLC differ more significantly than in the previous example. Figure 4 gives curves of  $\theta(\tau)$  obtained by integrating the ordinary differential equations (8) and by solving the partial differential equations (4) for  $\theta(\tau) \equiv \theta(\tau, L/2)$ . The boundary conditions for (4) were specified as in the previous case. The change in the  $z$ -component of the field was ignored, and the field amplitude was 5.5 times larger than the threshold value. Curve 2 in Fig. 4, plotted with

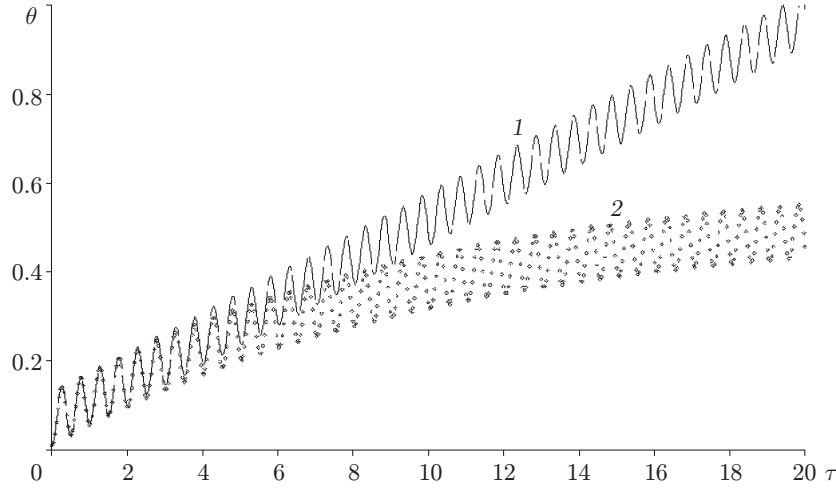


Fig. 4. Polar orientation angle of the 5SV NLC director versus dimensionless time [ignoring elasticity (1) and taking into account elasticity (2)] for the case of a circular electric field ( $\psi_x - \psi_z = \pi/2$  and  $\delta = 3$ ) lying in the plane  $(x, z)$ .

allowance for the elasticity of the medium, oscillates with the same frequency and amplitude, as curve 1, and, on the average, reaches the stationary level determined by the value of  $\delta$ , elastic constants, and crystal thickness  $L$ . As follows from numerical analysis (and qualitative considerations), the stationary level is reached always, even for an infinite excess of the field amplitude over the threshold magnitude.

The results of interaction of a NLC with a rotational field may be the basis for designing a high-frequency modulator (switch) of light using conventional “slow” NLC as the working medium.

The director rotation following from solution (14), was found experimentally. A NLC sample with diminished bond energy on the boundaries placed in an electric field orthogonal to the  $z$  axis (the electrode system on each surface was a configuration in the form of two or several parallel transparent bands, which in the assembly of the sample were perpendicular to each other) was exposed to a He-Ne laser, and the radiation transmitted through an analyzer was received by a photodiode. The voltage from one generator was supplied through a phase shift system to the electrodes of the sample. If necessary, transformers were switched into the tangential-field circuits to increase the field amplitude. At the moment when the phase difference of the applied electric fields approached  $\pi/2$ , the intensity of the transmitted radiation began to pulsate. The rotation period of the director was calculated from the oscillation period. The high-frequency component was appreciable up to  $\nu \sim 1$  MHz ( $\omega = 2\pi\nu$ ). Quantitative agreement within the framework of the simple model (9) was not obtained. In the experiment, we reliably detected pulsations of the transmitted radiation at a phase shift of the applied fields close to  $\pi/2$ , a sharp increase in the rotational velocity of the director with increase in the supplied voltage and, hence, its decrease with increase in the working frequency  $\omega$ . This result agrees qualitatively with the relations following from (14). The measurements were performed in the frequency range  $\nu = 10\text{--}5 \cdot 10^6$  Hz with an effective voltage of up to 50 V.

**Dynamics of Volume Orientation of NLCs. Numerical Calculation.** The solutions of system (8) for the general case were found using numerical calculations. The magnitudes of the electric fields for the initial homeotropic orientation were specified as

$$\begin{aligned} E_x &= E_{x0} \sin(2\pi\nu_x t + \psi_x), & E_y &= E_{y0} \sin(2\pi\nu_y t + \psi_y), \\ E_z &= \frac{\varepsilon_{\parallel} E_{z0} \sin(2\pi\nu_z t + \psi_z) - \varepsilon_a \sin\theta \cos\theta (E_x \cos\varphi + E_y \sin\varphi)}{\varepsilon_{\perp} + \varepsilon_a \cos^2\theta}. \end{aligned} \quad (16)$$

The  $z$  component of the field takes into account the anisotropic component following from condition (7) of the Maxwell equations;  $\omega_i = 2\pi\nu_i$ . For calculations, it is convenient to write (8) in dimensionless form:

$$\begin{aligned} \frac{d\theta}{d\tau} &= \delta(\mathbf{nA})(\mathbf{mA}), & \sin\theta \frac{d\varphi}{d\tau} &= \delta(\mathbf{nA})(\mathbf{pA}), \\ \theta(0) &= \theta_0, & \varphi(0) &= \varphi_0, \end{aligned} \quad (17)$$

TABLE 1

Table of Initial Parameters

Figure number	NLC Type	$a_x : a_y : a_z$	$\omega_x : \omega_y : \omega_z$	$\psi_x, \psi_y, \psi_z$	$\delta$
5, 7	MBBA	1 : 1 : 1	$2\pi(1.25 : 1 : 1)$	$0, \pi/2, 0$	-1.5
6, 10	5SV	1 : 1 : 1	1 : 1.1 : 1	$0, 0, \pi/2$	0.65
8, 9	5SV	1 : 1 : 1.5	$2\pi(1 : 1.1 : 1)$	$\pi/2, 0, 0$	30
11a	MBBA	1 : 1.1 : 1	$2\pi(1.25 : 1.1 : 1)$	$0, \pi/2, 0$	-5
11b	MBBA	1 : 1 : 1.06	$2\pi(1.2 : 1 : 1)$	$0, \pi/2, 0$	-2
11c	MBBA	1 : 1 : 1	$2\pi(1 : 1.1 : 1)$	$\pi/2, 0, 0$	-1.45

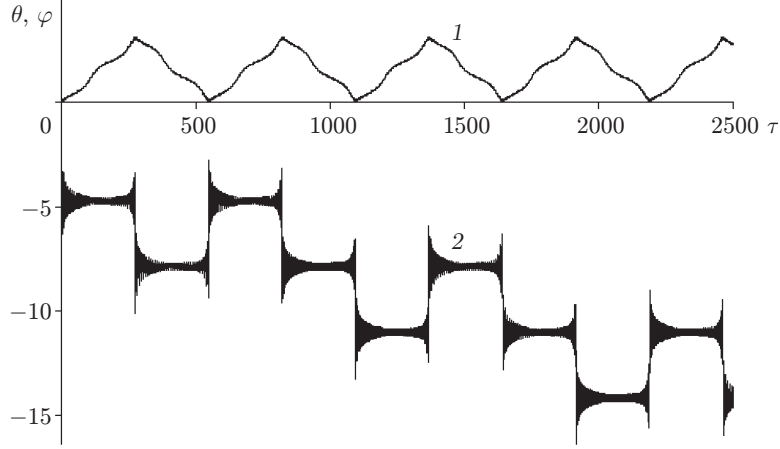


Fig. 5. Polar ( $\theta$ ) and azimuthal ( $\varphi$ ) orientation angles of the director versus dimensionless time (curves 1 and 2, respectively).

where  $\theta_0$  and  $\varphi_0$  are initial conditions. The normalizing factors are the root-mean-square amplitude of the field  $A = (E_{x0}^2 + E_{y0}^2 + E_{z0}^2)^{1/2}$  and the mean frequency  $\nu_0 = (\nu_x + \nu_y + \nu_z)/3$ . In this case,

$$\begin{aligned}
 A_x &= a_x \sin(2\pi N_x \tau + \psi_x), & A_y &= a_y \sin(2\pi N_y \tau + \psi_y), \\
 A_z &= \frac{\varepsilon_{||} a_z \sin(2\pi N_z \tau + \psi_z) - \varepsilon_a \sin \theta \cos \theta (A_x \cos \varphi + A_y \sin \varphi)}{\varepsilon_{\perp} + \varepsilon_a \cos^2 \theta},
 \end{aligned} \tag{18}$$

where  $a_x = E_{x0}/A$ ,  $a_y = E_{y0}/A$ ,  $a_z = E_{z0}/A$ ;  $N_x = \nu_x/\nu_0$ ,  $N_y = \nu_y/\nu_0$ ,  $N_z = \nu_z/\nu_0$ ;  $\psi_x, \psi_y$ , and  $\psi_z$  are phase additives,  $\tau = \nu_0 t$  is dimensionless time, and  $\delta = \varepsilon_a A^2 / (4\pi\gamma\nu_0)$  is a parameter.

The solutions of Eqs. (17) are diverse in nature. Depending on the parameters of the problem, the following regimes are observed: attainment of a stationary solution (an analog of the nonthreshold Freedericksz transition), periodic, quasiperiodic (multimode), and stochastic regimes of the strange attractor type. We consider several some dynamic regimes of orientation that provide a vivid illustration of the complexity of the calculated dependences. Along with the obtained functions  $\theta(\tau)$  and  $\varphi(\tau)$ , the motion of the end of the vector  $\mathbf{n}$  on a unit sphere or the motion trajectory plotted in the plane of  $\theta$  and  $\varphi$  (an analog of the phase space) provide a detailed picture of the behavior of the solution in time. The initial parameters used in the calculations and to plot the corresponding curves are presented in Table 1.

Below, we give solutions of system (17) for two types of NLC: 5SV ( $\varepsilon_a > 0$ ) and MBBA ( $\varepsilon_a < 0$ ). As can be seen from the figure, the behavior of the orientation in time is described by complex quasiperiodic and stochastic dependences similar to the strange attractor solutions [10]. Depending on the initial parameters, the director can have several limiting states (limiting cycles) [10]), around which it performed vibrational or rotational motion with periodic or quasiperiodic transitions from one cycle to another (Fig. 5). In the above example with a periodic change in the orientation state, the orientation angles are superimposed by a high-frequency component, whose amplitude increases considerably at the moment of transition from one state to another. The average values of neighboring levels in  $\varphi(\tau)$  differ from each other by the value  $\pm\pi$ , and the sign of the jump is accidental. The

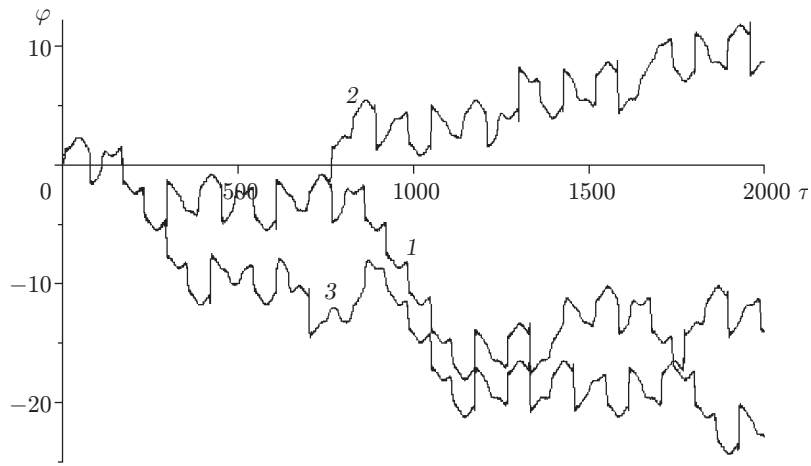


Fig. 6. Azimuthal angle  $\varphi$  versus dimensionless time  $\tau$  for various initial conditions: 1)  $\theta_0 = 0.001$  and  $\varphi_0 = 0$ ; 2)  $\theta_0 = 0.1$  and  $\varphi_0 = 0$ ; 3)  $\theta_0 = 0.1$  and  $\varphi_0 = 0.1$ .

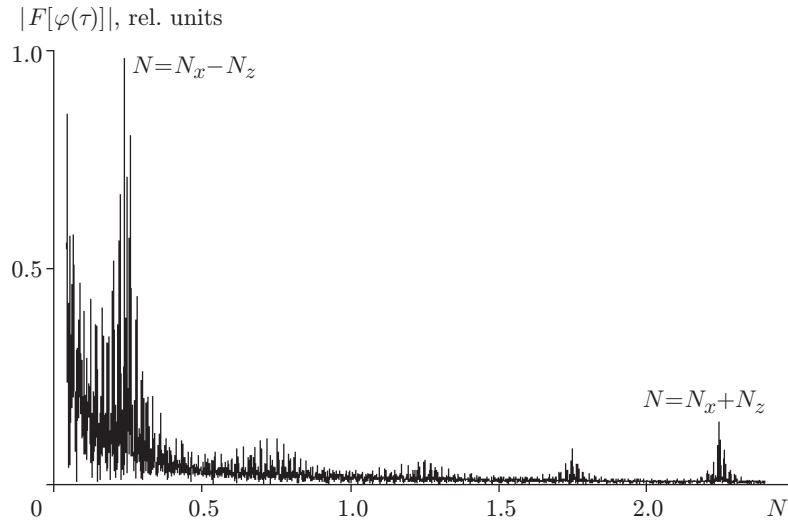


Fig. 7. Fourier spectrum  $|F[\varphi(\tau)]|$  versus dimensionless frequency.

maximum values of  $\theta(\tau)$  are reached at the tops of the triangles and are approximately equal to  $\pi/2$ . In contrast to  $\varphi(\tau)$ , the high-frequency amplitude of the function  $\theta(\tau)$  is more pronounced against the background of smoother variations.

In such regimes, the solutions of the equations begin to depend on the initial conditions. As an example, Fig. 6 gives curves of  $\varphi(\tau)$  [the dependence  $\theta(\tau)$  is not shown to save space] plotted for various conditions at the zero time  $\theta(0)$  and  $\varphi(0)$ . As can be seen from the figure, at a time close to  $\tau = 0$ , the course of the curves  $\varphi(\tau)$  for different initial conditions practically coincides, but at a certain time, the system “recollects” its initial state and sharply changes the motion trajectory. The behavior of the functions  $\theta(\tau)$  is similar.

The frequency spectrum versus the dimensionless frequency  $N = \nu/\nu_0$  (a Fourier image  $|F[\varphi(\tau)]|$ ) is chosen of nearly stochastic solutions becomes broadband; an example of the spectrum is given in Fig. 7. From the figure it is evident that in the regions of the difference frequency  $\Delta N = N_x - N_z$  and the total frequency  $N_x + N_z$  there are distinct peaks and the amplitude of the difference harmonics is approximately 8–10 times larger than that of the total harmonics. For large values of  $\delta$ , the time dependences  $\theta(\tau)$  and  $\varphi(\tau)$  become complicated and periodic in nature (Fig. 8). The Fourier spectrum (Fig. 9) becomes less dissected and have distinct equidistant harmonics spaced  $2\Delta N$  apart. The calculated transmission functions for a sample in a stochastic regime are more chaotic in



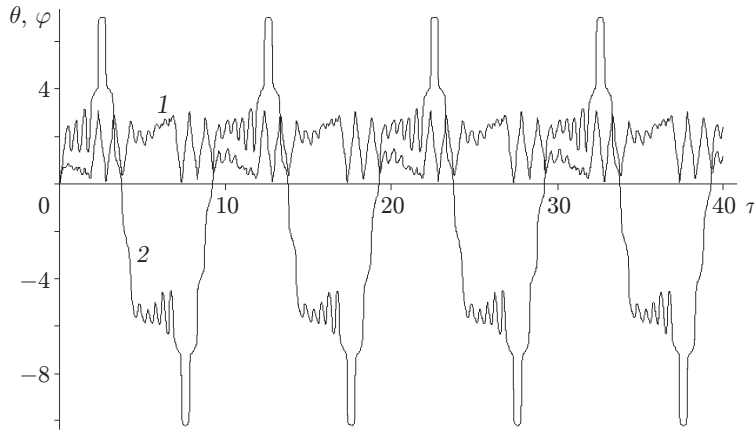


Fig. 8. Polar and azimuthal orientation angles of the director versus dimensionless time (curves 1 and 2, respectively).

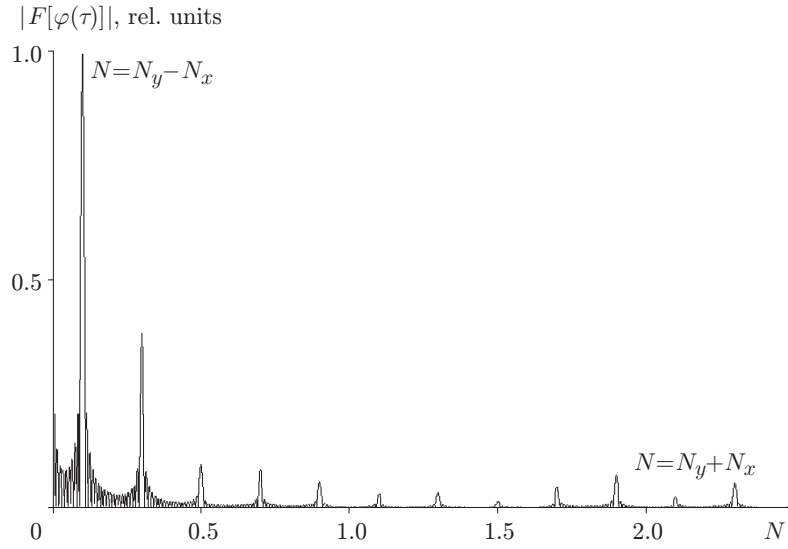


Fig. 9. Fourier spectrum  $|F[\varphi(\tau)]|$  versus dimensionless frequency.

appearance (Fig. 10) than the initial solutions  $\theta(\tau)$  and  $\varphi(\tau)$ . This is explained by additional nonlinear dependences in both the transmission function itself and in the general form [11]:

$$T(\tau) = T[\theta(\tau), \varphi(\tau)] = \cos^2 \chi - \sin 2\varphi \sin 2(\varphi - \chi) \sin^2(\Delta/2).$$

For our case, the phase advance difference  $\Delta$  is calculated by the formula

$$\Delta = 2\pi \frac{L}{\lambda} \left( \frac{n_{\perp} n_{\parallel}}{\sqrt{n_{\perp}^2 \cos^2 \theta + n_{\parallel}^2 \sin^2 \theta}} - n_{\perp} \right),$$

where  $\lambda$  is the wavelength of the normally incident diagnostic radiation,  $n_{\parallel}$  and  $n_{\perp}$  are the main values of the refraction index for the ordinary and extraordinary waves, respectively, and  $\chi$  is the angle between the polarizer and analyzer for the polarizer direction along the  $x$  axis.

The motion trajectories on a plane in the phase space are given in Fig. 11. As well as the functions  $\theta(\tau)$  and  $\varphi(\tau)$ , the given curves are rather complex in shape.

We note that the given solutions do not exhaust all kinds of dynamic behavior of the orientation obtained from (17). It is impossible to give the full set of regimes within the scope of one article, first of all because of a large number of initial parameters (in our case taking into account normalization, they are seven).

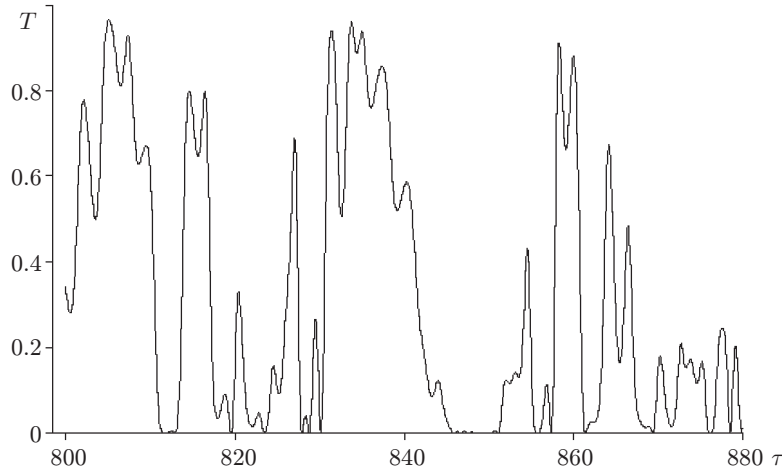


Fig. 10. Fragment of the transmission function versus dimensionless time.

Preliminary analysis shows that obtaining nondeterministic solutions requires, first of all, the presence of volume deformation of the NLC orientation or the presence of all three components of the field  $E_x \neq 0$ ,  $E_y \neq 0$ , and  $E_z \neq 0$ . This conclusion also follows from the mathematical statement on the absence of stochastic solutions in the systems described by one ordinary differential equation of the first order with an explicit time dependence [10]. In the absence of one of the field components  $E_i = 0$  ( $i = x, y, z$ ), system (8) in the steady-state regime reduces to one equation for the deflection angle of the director lying in the plane of variation of  $\mathbf{E}$ . In addition, in the radio frequency range, it is necessary that the electric fields contain components that have at least two different frequencies:  $\omega_i \neq \omega_j = \omega_k$  ( $i, j, k = x, y, z$ ;  $i \neq j \neq k$ ). This requirement can be violated if the NLC is exposed to a light radiation because the nonlinear relation between the ordinary and extraordinary waves inside the crystal is more complex than condition (7) [7]. A more detailed consideration of this problem is beyond the scope of the present paper.

The experiments performed in the radio frequency range confirm the theoretical conclusions on the existence of deterministic and stochastic regimes in the orientation of the NLC director. In these experiments, unlike in experiments with a single-frequency electric field lying in one plane, two independent generators were used and the electrode circuit of the sample allowed fields to be produced in three orthogonal directions. In the experiments, the diagnostic radiation was focused into the sample and then projected onto a remote matte screen. At the moment of occurrence of instability, a region of time-varying light intensity or several regions pulsating almost independently of each other formed in the light spot. In this case, the intensity of the entire spot integrated over the cross section remained unchanged or oscillated weakly in time. Visually, the pulsation region became uniformly illuminated and depolarized. All external changes depended on the position of the point through which the diagnostic radiation transmitted, time, and temperature.

The experimental transmission curve  $T(t)$  given in Fig. 12 was obtained as follows (the parameters of the 5SV sample  $10 \mu\text{m}$  thick and the external fields correspond to the conditions of Fig. 6). The magnified light spot was superimposed by a diaphragm with a small opening, behind which there was a photodiode (or a photoelectron multiplier) connected to a recording device. The recorded transmission curves outwardly resemble a stochastic regime and depend on the position of the center of the diaphragm on the spot. Similar phenomena were observed in the previous simpler cases of a single-frequency, in-plane rotating field.

**Discussion of Results.** Analysis of the transmission function did not yield quantitative agreement between calculation and experimental data. The main reason for the differences lies in ignoring the spatial dependence of the electric fields, the possibility of occurrence of hydrodynamic flows (as a result of low-frequency components in the orientation dynamics), and flexoelectric effects. We note that accounting for the spatial dependence of the orientation  $\mathbf{n}$  by numerical integration of the partial differential equations (4) and (7) led to even greater complexity and diversity of solutions.

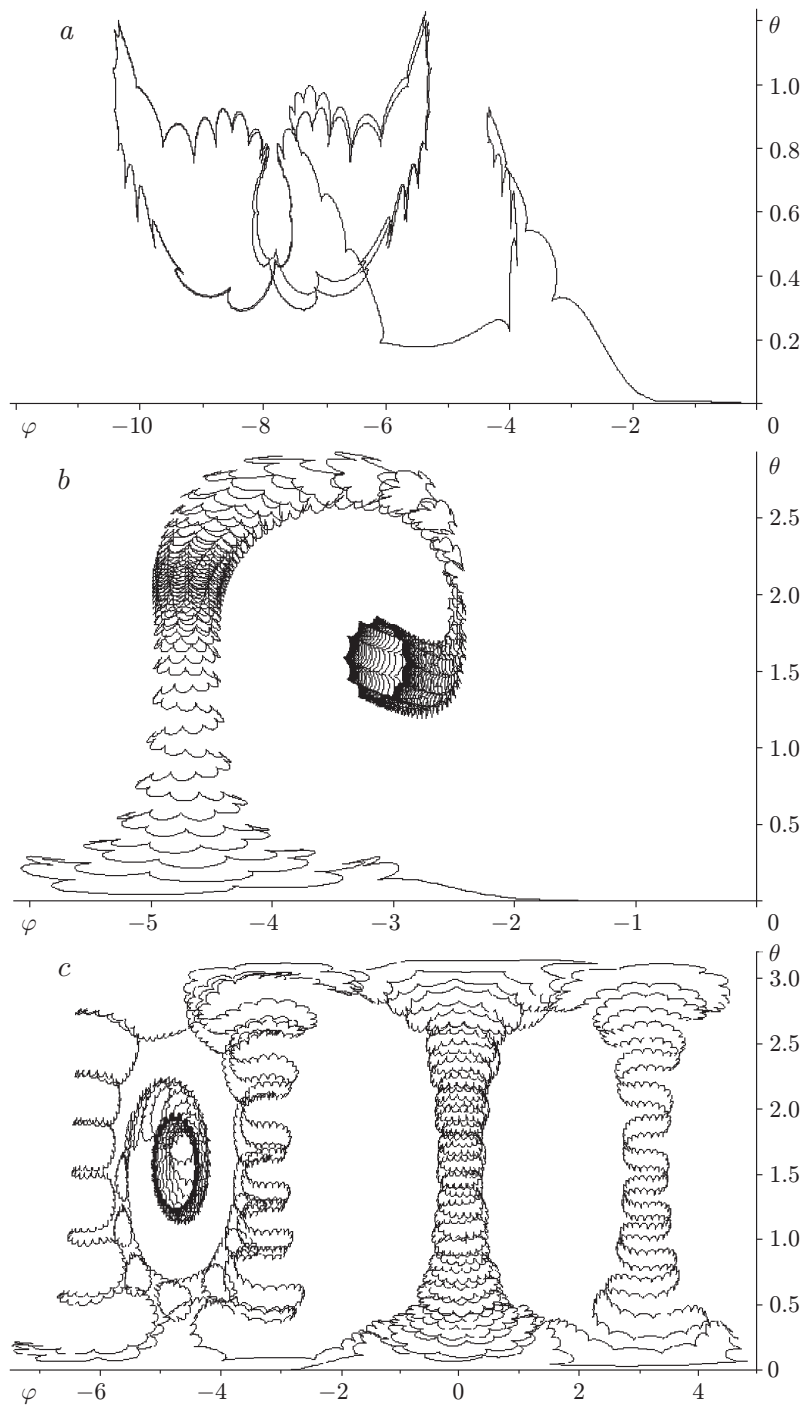


Fig. 11. Motion trajectory on the plane  $(\theta(\tau), \varphi(\tau))$ .

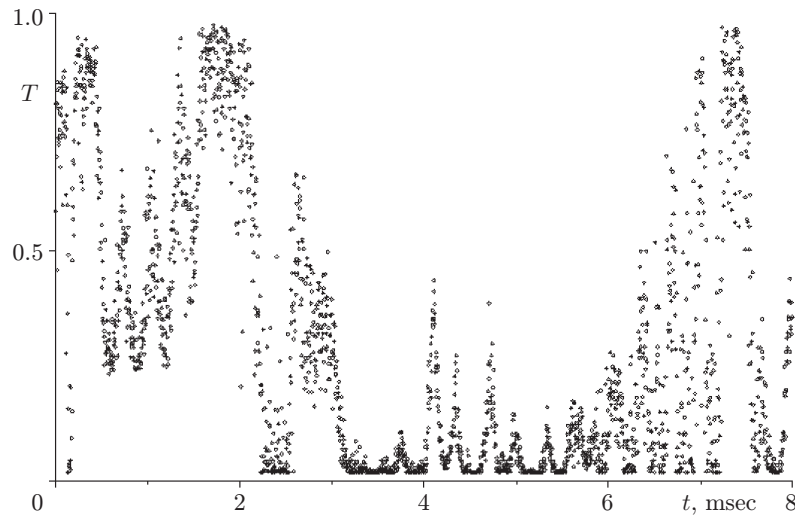


Fig. 12. Transmission function  $T(t)$  obtained in the experiment (parameters the same as in Fig. 6).

After a proper change of variables, the discrete version of the particular case of Eqs. (17) and (18) becomes the sequence studied in [12]. The equations leading to this sequence provides an approximate description of the system of three nonlinear interrelated oscillators. In this case, the constructed Poincaré sections are maps of an abstract torus in the four-dimensional phase space  $(\dot{\theta}, \dot{\varphi}, \theta, \varphi)$  onto a two-dimensional plane. In [12], the presence of chaotic attractor solutions is proved by numerical calculations and the constructed motion trajectories are similar in complexity to the sections obtained in the present study.

The specificity of the attractor behavior of the solutions and the high sensitivity of the discrete version of the equations to the initial conditions and input parameters (for example, in [12], the amplitude and phase additives in (18) were chosen in a random manner) did not allowed us to make a precise quantitative comparison of the results of [12] with the calculations of the present study.

In conclusion, we note that the present research was motivated by studies in the area of harmonic generation during interaction of polymer media with coherent radiation. This issue for liquid crystals has been studied experimentally [13, 14] and theoretically [15]. In the cited studies there was a considerable spread in experimental data. In [15], the generation of the second harmonic of NLCs was treated as a consequence of the Ericksen–Leslie continuum equations and the Maxwell equations. The disturbance of the central symmetry that arose in that case was explained by the light-induced deformation of the crystal structure. The solution obtained in [15] was the result of a linear approximation and did not completely reflect the entire process involved in this interaction. The attempt of the authors of the present paper to numerically study the nonlinear interaction regimes of multiwave radiation with NLCs gave an unexpected result. From analysis of the factors responsible for seemingly nonphysical solutions, it was concluded that this effect is due to the properties of NLC media, which are described by constitutive equations. In view of this, a simplified mathematical model was chosen (modified Maxwell equations), which is nevertheless close to the model of interaction of NLCs with radio frequency alternating electric fields.

**Conclusions.** The studies performed revealed a physical object of nonlinear dynamics — an NLC in a multicomponent alternating electric field. This object was described by a dissipative system of ordinary differential equations, which is one more example of the well-known deterministic equations leading to chaotic oscillations [10]. In view of this, the possibility of stochastization of the orientational state of NLCs should be taken into account in considering the interaction of liquid-crystal media with multicomponent and multifrequency electric fields.

We thank G. N. Grachev for support in the experiments and the work as a whole and V. F. Kitaeva and A. S. Zolot'ko from the Lebedev Physical Institute of the Russian Academy of Sciences for useful discussions.

## REFERENCES

1. L. M. Blinov, *Electro- and Magneto-Optics of Liquid Crystals* [in Russian], Nauka, Moscow (1978).
2. Khoo Iam-Choon, *Liquid Crystals*, Wiley, New York (1995).
3. V. V. Belayev, *Viscosity of Nematic Liquid Crystals* [in Russian], Fizmatlit, Moscow (2002).
4. S. A. Pikin, *Structural Transformations in Liquid Crystals* [in Russian], Nauka, Moscow (1981).
5. N. V. Tabiryan, A. V. Sukhov, and B. Y. Zel'dovich, "The orientational optical nonlinearity of liquid crystals," *Mol. Cryst. Liq. Cryst.*, **136**, 1–139 (1986).
6. A. S. Zolot'ko, V. F. Kitaeva, N. Kroo, et al., "Undamped oscillations of the NLC director in the field of an ordinary light wave," *Zh. Éksp. Teor. Fiz.*, **87**, 859–864 (1984).
7. N. G. Preobrazhenskii and S. I. Trashkeev, "Multimode oscillations of the nematic liquid crystal director in the light field of an oblique o-wave," *Opt. Spectroscop.*, **62**, 1404–1407 (1987).
8. A. S. Zolot'ko, V. F. Kitaeva, N. N. Sobolev, et al., "Polarization dynamics of an ordinary light wave interacting with a nematic liquid crystal," *Liquid Crystal*, **15**, No. 6, 787–797 (1993).
9. A. Vella, B. Piccirilo, and E. Santamoto, "Coupled-mode approach to the nonlinear dynamics induced by an elliptically polarized laser field in liquid crystals at normal incidence," *Phys. Rev. E*, **65**, 1–7 (2002).
10. F. C. Moon, *Chaotic Vibrations*, Wiley, Chichester (1987).
11. M. Born and E. Wolf, *Principles of Optics*, Pergamon, London (1970).
12. C. Grebogy, E. Ott, and J. A. Yorke, "Attractors on an N-Torus: Quasiperiodicity versus chaos," *Physica*, **15D**, 354–373 (1985).
13. M. I. Barnik, L. M. Blinov, A. M. Dorozhkin, et al. "Optical 2ND harmonic-generation in various liquid-crystalline phases," *Mol. Cryst. Liq. Cryst.*, **98**, 1–12 (1983).
14. S. M. Arakelyan and Yu. S. Chiligaryan, *Nonlinear Optics of Liquid Crystals* [in Russian], Nauka, Moscow (1984).
15. Ou-Yang Zhong-can and Xie Yu-zhang, "Theory of second-harmonic generation in nematic liquid crystals," *Phys. Rev.*, **32**, No. 2, 1189–1200 (1985).